ACS APPLIED MATERIALS & INTERFACES

Research Article

www.acsami.org

Directed Self-Assembly of Silicon-Containing Block Copolymer Thin Films

Michael J. Maher,[†,‡] Charles T. Rettner,[‡] Christopher M. Bates,[†] Gregory Blachut,[§] Matthew C. Carlson,[§] William J. Durand,[§] Christopher J. Ellison,[§] Daniel P. Sanders,[‡] Joy Y. Cheng,[*,‡] and C. Grant Willson[*,†,§]

[†]Department of Chemistry and [§]McKetta Department of Chemical Engineering, The University of Texas at Austin, Austin, Texas 78712, United States

[‡]IBM Research—Almaden, 650 Harry Road, San Jose, California 95120, United States

Supporting Information

ABSTRACT: The directed self-assembly (DSA) of lamella-forming poly(styrene-*block*-trimethylsilylstyrene) (PS−PTMSS, L_0 = 22 nm) was achieved using a combination of tailored top interfaces and lithographically defined patterned substrates. Chemo- and grapho-epitaxy, using hydrogen silsesquioxane (HSQ) based prepatterns, achieved density multiplications up to 6× and trench space subdivisions up to 7×, respectively. These results establish the compatibility of DSA techniques with a high etch contrast, Si-containing BCP that requires a top coat neutral layer to enable orientation.

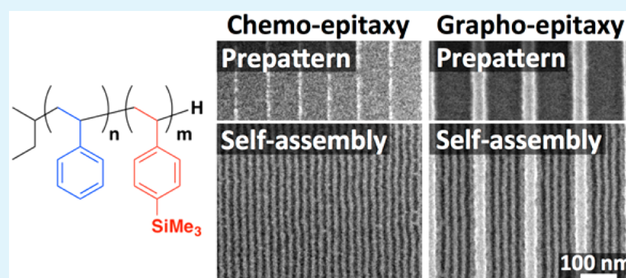

KEYWORDS: *directed self-assembly, block copolymers, lithography, chemo-epitaxy, grapho-epitaxy, top coats*

INTRODUCTION

Nanostructures formed from block copolymer (BCP) self-assembly are being applied in fields such as photonics,[1] polymer electrolyte membranes,[2] nanofiltration,[3] and next-generation lithography.[4] Further advances in nanomanufacturing applications, such as bit patterned media for hard disk drives[5] and semiconductor device manufacturing, require establishing methods for patterning sub-10 nm features (e.g., lamellae or cylinders). This length scale is beyond the resolution limit of both photolithography and BCP self-assembly using poly(styrene-*block*-methyl methacrylate) (PS−PMMA). High-χ BCPs (i.e., polymers with a large interaction parameter, χ) can form sub-10 nm domains,[6−9] but the low etch contrast of typical organic−organic BCPs becomes a challenge as the dimensions approach 10 nm. Organic polymers that contain inorganic constituents, such as silicon,[10−13] are inherently etch resistant.[14] Hence, incorporation of one such block in high-χ BCPs affords exceptional etch contrast. However, the directed self-assembly (DSA) of lamella-forming, Si-containing BCPs has not been studied in detail because the lower surface energy Si-containing block segregates to the top interface during thermal annealing and thereby drives a parallel orientation of the domains.[15] For patterning applications, a perpendicular orientation of the lamellae is required along with controlled lamella placement and alignment (Herein, orientation refers to the direction normal to the substrate interface and alignment refers to the direction in the plane of the film). Thermal annealing is preferred because it can rapidly orient the BCP domains and is compatible with existing industrial processes. Therefore, orientation and alignment control via thermal annealing is preferred for high-resolution patterning.

The orientation of BCP domains is controlled by interfacial interactions. Preferential interactions between a block and either the substrate or top interface result in a parallel orientation. Nonpreferential ("neutral") interactions promote a perpendicular orientation of BCP domains,[16] which is the orientation needed for pattern transfer. Substrate surface treatments comprised of random copolymers have been reported to provide a neutral layer and enable the perpendicular orientation of BCPs.[17−22] Recently, these principles have been extended to the top interface,[23−27] which has enabled orientation control over diverse classes of BCPs via thermal annealing. Descriptions of the material synthesis, optimization, and definitive characterization of (non)preferential top and bottom interfacial interactions have been reported.[28−31]

To various degrees of success, achieving the long-range order of BCP domains has been reported through use of in-plane electric fields,[32] heterogeneous surfaces,[33] temperature gradients,[34] topographic prepatterns (grapho-epitaxy),[35,36] and chemical prepatterns (chemo-epitaxy).[37−39] These latter two methods are the leading candidates for DSA because: (1) registration of the BCP domains with low placement error is possible,[40] (2) self-aligned customization can afford complex device-oriented patterns[41−43] of the sort required to produce fully functioning Fin-FET devices,[44] and (3) both processes are

Received: November 21, 2014
Accepted: January 16, 2015
Published: January 16, 2015

ACS Publications © 2015 American Chemical Society

DOI: 10.1021/am508197k
ACS Appl. Mater. Interfaces 2015, 7, 3323−3328

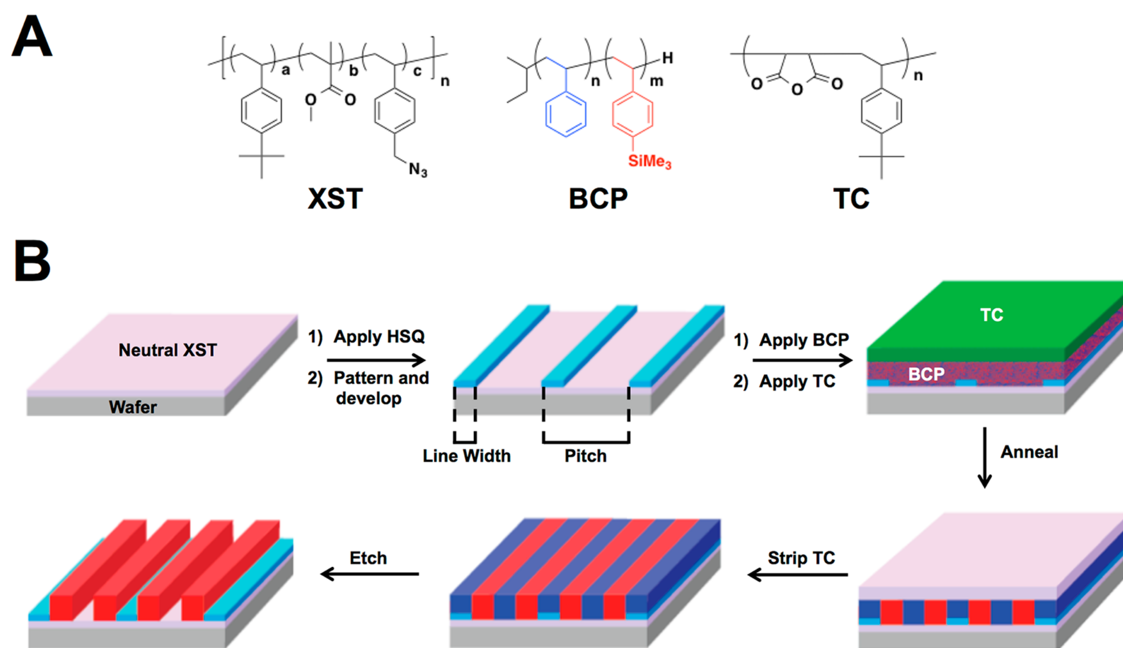

Figure 1. (A) Materials used in the present study. (B) Schematic of the chemo-epitaxy strategy using HSQ directing lines.

compatible with 193 nm immersion lithography[45,46] and can be integrated with 300 mm state-of-the-art processes for high-volume manufacturing.[47−50]

Chemo-epitaxy, grapho-epitaxy, or a combination of both can be used to accomplish various patterning goals within the microelectronics industry. Each method has certain advantages and disadvantages. Chemo-epitaxy has much stricter patterning requirements and relies on the ability pattern chemical guide lines on the order of BCP periodicity, L_0 (guidelines between 0.5 and 1.5L_0 are used for DSA). This will be a major challenge as the BCP periodicity is reduced to sub-15 nm. Grapho-epitaxy has less strict patterning requirements than the chemo-epitaxy approach because it subdivides a larger patterned area. However, the physical prepatterns occupy valuable space on the wafer, which makes chemo-epitaxy more attractive for certain applications.

The majority of DSA research and development has been done with PS−PMMA because the free surface (in air, nitrogen, or vacuum) is energetically neutral to the components of the BCP at elevated temperatures,[51] which enables the formation of perpendicular features when annealed on neutral layer alone. PS−PMMA also has acceptable etch selectivity because the PMMA component is particularly sensitive to ion bombardment.[52] Unfortunately, PS−PMMA suffers from a relatively small χ and can only form a minimum half-pitch of approximately 10−12 nm.[53] As previously stated, high-χ BCPs that contain only organic components are unlikely to have the same intrinsic etch selectivity as PS−PMMA. Recently, Carlson et al. introduced a family of silicon-containing BCPs including poly(styrene-*block*-trimethylstyrene) (PS−PTMSS), poly(styrene-*block*-pentamethyldisilylstyrene) (PS−PDSS), and poly(4-methoxystyrene-*block*-trimethylstyrene) (PMOST−PTMSS) as candidates for lithographic applications.[54] These BCPs can be oriented using top coats. They are highly etch resistant and can form features as small as 7 nm. The first DSA work on this class of BCPs is reported herein using lamella-forming PS−PTMSS (L_0 = 22 nm) as a model. DSA was accomplished by combining well-established chemo- and grapho-epitaxy techniques in conjunction with top coats for orientation control. These strategies should be applicable to the other BCPs in this family. Hydrogen silsesquioxane (HSQ) was used to direct the self-assembly because it is a negative-tone e-beam resist compatible with sub-10 nm patterning[55] and has been previously used for both chemo[40,56]and grapho[44]-epitaxy of PS−PMMA.

RESULTS AND DISCUSSION

Figure 1A illustrates the materials used in the present study (full characterization is reported elsewhere[31]), and Figure 1B shows the process flow used for the chemo-epitaxy approach. A polymeric surface treatment (XST) comprised of a random copolymer of 4-*tert*-butylstyrene, methyl methacrylate, and 4-vinylbenzylazide was thermally cross-linked on a substrate. HSQ was spin coated on the neutral surface, patterned using e-beam lithography, and developed to achieve lines of approximately 0.5L_0 (11 nm). In the figure, a 2L_0 HSQ full pitch (0.5L_0 HSQ line + 1.5L_0 space) pattern is illustrated. The BCP was spin coated onto the chemically patterned surface and the trimethylamine salt of a poly(4-*tert*-butylstyrene-*alt*-maleic anhydride) top coat (TC) was spin coated on top of the BCP using an orthogonal solvent, methanol.[31] Thermal annealing induces a polarity switch in the TC, which produces a neutral top interface and facilitates the formation of perpendicular lamellae.[24] Interestingly, the HSQ lines have a higher affinity for the PS block than the PTMSS block, which caused the PS domains to segregate over the HSQ covered regions (as will be discussed later). This directing interaction induced the alignment of the PS domains and the adjacent domains overlaying the nonpreferential region (XST region, which is not covered by HSQ) of the substrate. After annealing, the TC was removed by washing with tetramethylammonium hydroxide (TMAH) based developer. Finally, for inspection purposes, O_2 reactive ion etching was performed to selectively remove the PS domains, enabling observation of the line/space pattern by SEM.

DOI: 10.1021/am508197k
ACS Appl. Mater. Interfaces 2015, 7, 3323−3328

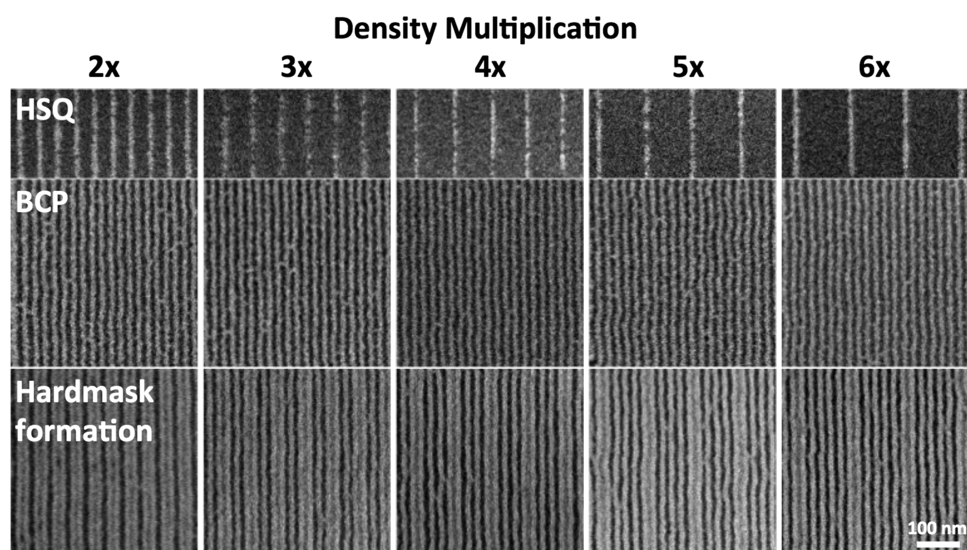

Figure 2. SEMs of HSQ guide lines (top), self-assembled BCP (middle), and hardmask after further etching (bottom). The BCP (thickness = $1L_0$, 22 nm) was annealed for 10 min at 190 °C. The scale bar is valid for all micrographs.

Three parameters were varied to optimize the DSA process shown in Figure 1B: HSQ line width, HSQ pitch, and the composition of the XST. It was found that integer (n) multiples of 22.5 nm (within 3% of L_0) successfully induced alignment. The range of HSQ line widths that successfully directed assembly was found to be between 10 and 12 nm (approximately $0.5L_0$). Additionally, the composition of the XST was varied, and a slightly off-neutral composition was found to minimize defectivity (see Figure S1 in the Supporting Information). There was unequal block coverage in the interstitial regions between HSQ guidelines. Because HSQ is preferential for the PS block, the interstitial region contained excess PTMSS block. Therefore, a slightly PTMSS preferential XST was chosen, which produced optimum alignment. A similar phenomenon has been reported in the chemo-epitaxy of PS−PMMA.[57]

Figure 2 (top row) shows the HSQ guidelines at various pitches corresponding to near-integer multiples of the BCP periodicity, L_0. The HSQ dimensions were measured in reference to the BCP periodicity and determined to be approximately 0.5 L_0 (10−12 nm, Table S1 in the Supporting Information). The height of the HSQ lines was approximately 5 nm (see Figure S2 in the Supporting Information) as measured by atomic force microscopy (AFM). The as-cast thickness of the BCP layer was ca. $1L_0$ (22 nm) and the as-cast thickness of TC was ca. 20 nm. The samples were thermally annealed at 190 °C in air for 10 min. Figure 2 (middle row) shows the corresponding BCP domain pattern after the TC was removed using a TMAH-based developer and developed with a subsequent oxygen etch. The BCP alignment is near perfect across the entire patterned area (3 μm × 4 μm) with density multiplications ≤4×. It is likely that the minor bridging observed between the BCP domains can be improved by optimization of the etch process. This hypothesis is supported by the excellent PS−PTMSS structures recently produced using advanced etch tools with highly optimized recipes.[31] At 5× and 6× density multiplications, the BCP alignment contained minor dislocations and disclinations, and the frequency of these defects scaled with the density multiplication. Some of these defects are highlighted in the larger area images provided in the Supporting Information (Figure S3−S4). The results are on par with chemo-epitaxy density multiplications reported elsewhere.[58,59]

Unlike previous efforts using HSQ-based chemical patterns to direct PS−PMMA,[40,56] it was not intuitively obvious which domain would be preferentially directed by the HSQ lines as neither the PS nor the PTMSS domains have polar or hydrogen bonding groups, which would strongly interact with the oxide-like HSQ lines. Figure 2 (bottom row) shows the hardmask after etching completely through the PS domain and the neutral layer. The most notable feature is the appearance of alternating lines that are either 11 or 33 nm wide. The 33 nm line arises from the apparent fusion of the HSQ and the two adjacent PTMSS domains (both HSQ and PTMSS contain oxidized silicon after exposure to O_2 RIE). Because the PS block located on the HSQ is removed, the exposed HSQ and two flanking PTMSS domains appear as a single "fused" domain as observed from the top-down. These data confirm that the HSQ has preferential affinity for the PS domains (which are less hydrophobic than the PTMSS domains). If PTMSS domains were aligned on top of the HSQ line, no 33 nm line would be observed, and Figure 2 (middle) and Figure 2 (bottom) would be identical.[40,42]

Grapho-epitaxy was also studied and demonstrated using trenches formed from HSQ. The process flow is outlined in Figure 3. Preparation of samples was similar to the chemo-epitaxy flow with several slight modifications. First, the XST was not purposefully skewed to favor the PTMSS block. Instead, a perfectly neutral XST was used as previously reported.[31] Second, a far thicker layer of HSQ was used to form the physical prepatterns. The result is a neutral surface bordered by PS preferential sidewalls that are taller than the thickness of the block copolymer. The trench subdivision is defined as the number of natural periods that span the width of the trench.

Figure 4 (top row) shows the physical trenches that were formed by patterning HSQ. The trenches are approximately 40 nm deep (see Figure S5 in the Supporting Information). BCP was spin-coated to partially fill the trench with BCP. Then, the sample was coated with top coat and annealed. The top coat was stripped, and the sample was etched. Figure 4 (bottom row) shows micrographs of 3×, 5×, and 7× DSA subdivision of

DOI: 10.1021/am508197k
ACS Appl. Mater. Interfaces 2015, 7, 3323−3328

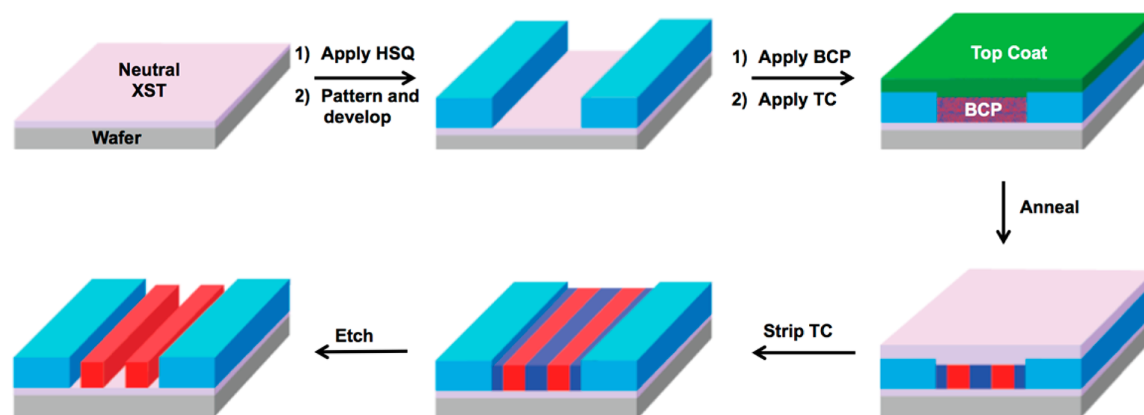

Figure 3. Schematic of the grapho-epitaxy flow using HSQ trenches.

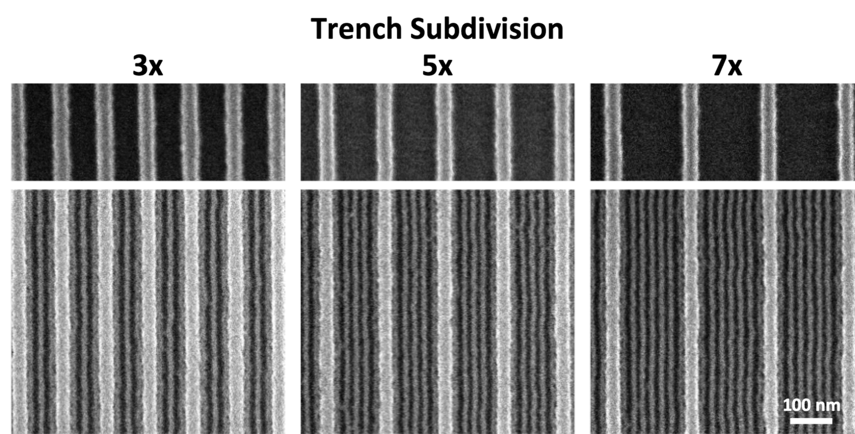

Figure 4. SEM micrographs of HSQ trenches (top) and grapho-epitaxy of the BCP (bottom). The scale bar is valid for all micrographs.

HSQ trenches. In this example, the thickness of the BCP was approximately 25 nm (see Figures S5 and S6 in the Supporting Information). The DSA is near perfect with trench subdivisions ≤5×. At larger trench subdivisions, such as 7×, the system accommodates more defects, examples of which are highlighted in the larger area SEM images (see Figure S7 in the Supporting Information). Trenches that were commensurate in width (within approximately 5% of L_0, Table S2 in the Supporting Information) to the natural periodicity were found to direct the alignment. Trenches incommensurate with the natural periodicity showed higher levels of defects and did not direct the alignment, which is in agreement with literature reports.[60]

The quality of the DSA patterns produced by chemo-epitaxy and grapho-epitaxy are very similar. No significant qualitative differences were observed, which is important because it demonstrates that the class of BCP used herein is amenable to DSA via both leading techniques. Future work involves larger area demonstrations, integration with 193 nm lithography, and quantification of the defectivity, line-edge roughness, line-width roughness, and placement error.

CONCLUSION

The work presented herein extends chemo- and grapho-epitaxy (DSA alignment control) to Si-based BCPs, which require top coats to control the top interface. Chemo- and grapho-epitaxy of vertically oriented lamellae from PS−PTMSS produced density multiplications and trench subdivision up to 6× and 7×, respectively. The combination of orientation control afforded by tailored top/bottom interfacial materials and epitaxially induced alignment provides a satisfying demonstration of the potential for this process to extend DSA beyond the limits of PS−PMMA. Full integration of high-resolution BCP patterning of this sort with large-scale manufacturing is within reach, and the author's hope that extension of the underlying patterning methodologies to next-generation technology nodes will be facilitated by the principles, materials, and techniques described in this manuscript.

ASSOCIATED CONTENT

Supporting Information

Experimental procedures, Figures S1−S7, and Tables S1−S2. This material is available free of charge via the Internet at http://pubs.acs.org.

AUTHOR INFORMATION

Corresponding Authors

*E-mail: chengjo@us.ibm.com.
*E-mail: willson@che.utexas.edu.

Notes

The authors declare no competing financial interest.

ACKNOWLEDGMENTS

The authors thank Nissan Chemical Industries, Lam Research, the ASTC, and the National Science Foundation (Grants EECS-1120823 and EEC-1160494) for financial support. M.J.M. thanks the IBM Ph.D. Fellowship Program and the National Science Foundation Graduate Research Fellowship (Grant DGE-1110007) for financial support. G.B. thanks the

DOI: 10.1021/am508197k
ACS Appl. Mater. Interfaces 2015, 7, 3323−3328

Paul D. Meek Endowed Graduate Fellowship in Engineering for support. W.J.D. thanks the Virginia and Ernest Cockrell, Jr. Fellowships in Engineering for partial support. C.J.E. thanks the Welch Foundation (Grant #F-1709) for partial financial support. G.W. thanks the Rashid Engineering Regents Chair and the Welch Foundation (Grant #F-1830) for partial financial support. The authors also thank Jane Frommer for AFM assistance, Elizabeth Lofano for SEM assistance, and Amy Bowers for etch assistance. The authors thank Dustin Janes for stimulating conversations. Any opinion, findings, and conclusions or recommendations expressed in this material are those of the authors and do not necessarily reflect the views of the National Science Foundation or the sponsors.

REFERENCES

(1) Miyake, G. M.; Piunova, V. A.; Weitekamp, R. A.; Grubbs, R. H. Precisely Tunable Photonic Crystals From Rapidly Self-Assembling Brush Block Copolymer Blends. *Angew. Chem., Int. Ed.* **2012**, *51*, 11246−11248.

(2) Schulze, M. W.; McIntosh, L. D.; Hillmyer, M. A.; Lodge, T. P. High-Modulus, High-Conductivity Nanostructured Polymer Electrolyte Membranes via Polymerization-Induced Phase Separation. *Nano Lett.* **2014**, *14*, 122−126.

(3) Jackson, E. A.; Hillmyer, M. A. Nanoporous Membranes Derived From Block Copolymers: From Drug Delivery to Water Filtration. *ACS Nano* **2010**, *4*, 3548−3553.

(4) Bates, C. M.; Maher, M. J.; Janes, D. W.; Ellison, C. J.; Willson, C. G. Block Copolymer Lithography. *Macromolecules* **2014**, *47*, 2−12.

(5) Albrecht, T. R.; Bedau, D.; Dobisz, E.; Gao, H.; Grobis, M.; Hellwig, O.; Kercher, D.; Lille, J.; Marinero, E.; Patel, K.; Ruiz, R.; Schabes, M. E.; Wan, L.; Weller, D.; Wu, T. Bit Patterned Media at 1 Tdot/in^2 and Beyond. *IEEE Trans. Magn.* **2013**, *49*, 773−778.

(6) Keen, I.; Yu, A.; Cheng, H.-H.; Jack, K. S.; Nicholson, T. M.; Whittaker, A. K.; Blakey, I. Control of the Orientation of Symmetric Poly (Styrene)-Block-Poly(D,L-lactide) Block Copolymers Using Statistical Copolymers of Dissimilar Composition. *Langmuir* **2012**, *28*, 15876−15888.

(7) Kim, S.; Nealey, P. F.; Bates, F. S. Decoupling Bulk Thermodynamics and Wetting Characteristics of Block Copolymer Thin Films. *ACS Macro Lett.* **2012**, *1*, 11−14.

(8) Li, H.; Gu, W.; Li, L.; Zhang, Y.; Russell, T. P.; Coughlin, E. B. Synthesis of Semicrystalline/Fluorinated Side-Chain Crystalline Block Copolymers and Their Bulk and Thin Film Nanoordering. *Macromolecules* **2013**, *46*, 3737−3745.

(9) Kennemur, J. G.; Yao, L.; Bates, F. S.; Hillmyer, M. A. Sub-5 nm Domains in Ordered Poly(cyclohexylethylene)-*block*-poly(methyl methacrylate) Block Polymers for Lithography. *Macromolecules* **2014**, *47*, 1411−1418.

(10) Jung, Y.-S.; Ross, C. A. Orientation-Controlled Self-Assembled Nanolithography Using a Polystyrene-Polydimethylsiloxane Block Copolymer. *Nano Lett.* **2007**, *7*, 2046−2050.

(11) Cushen, J. D.; Otsuka, I.; Bates, C. M.; Halila, S.; Fort, S.; Rochas, C.; Easley, J. A.; Rausch, E. L.; Thio, A.; Borsali, R.; Willson, C. G.; Ellison, C. J. Oligosaccharide/Silicon-Containing Block Copolymers with 5 nm Features for Lithographic Applications. *ACS Nano* **2012**, *6*, 3424−3433.

(12) Bates, C. M.; Pantoja, M. A. B.; Strahan, J. R.; Dean, L. M.; Mueller, B. K.; Ellison, C. J.; Nealey, P. F.; Willson, C. G. Synthesis and Thin-Film Orientation of Poly(styrene- *block*-trimethylsilylisoprene). *J. Polym. Sci., Part A: Polym. Chem.* **2012**, *51*, 290−297.

(13) Cushen, J. D.; Bates, C. M.; Rausch, E. L.; Dean, L. M.; Zhou, S. X.; Willson, C. G.; Ellison, C. J. Thin Film Self-Assembly of Poly(Trimethylsilylstyrene-*b*-D,L-Lactide) with Sub-10 nm Domains. *Macromolecules* **2012**, *45*, 8722−8728.

(14) Jurgensen, C. W.; Shugard, A.; Dudash, N.; Reichmanis, E.; Vasile, M. J. Experimental Tests of the Steady-State Model for Oxygen Reactive Ion Etching of Silicon-Containing Polymers. *J. Vac. Sci. Technol., A* **1988**, *6*, 2938−2944.

(15) Andersen, T. H.; Tougaard, S.; Larsen, N. B.; Almdal, K.; Johannsen, I. Surface Morphology of PS−PDMS Diblock Copolymer Films. *J. Electron Spectrosc. Relat. Phenom.* **2001**, *121*, 93−110.

(16) Walton, D. G.; Kellogg, G. J.; Mayes, A. M.; Lambooy, P.; Russell, T. P. A Free Energy Model for Confined Diblock Copolymers. *Macromolecules* **1994**, *27*, 6225−6228.

(17) Ryu, D. Y.; Shin, K.; Drockenmuller, E.; Hawker, C. J.; Russell, T. P. A Generalized Approach to the Modification of Solid Surfaces. *Science* **2005**, *308*, 236−239.

(18) In, I.; La, Y.-H.; Park, S.-M.; Nealey, P. F.; Gopalan, P. Side-Chain-Grafted Random Copolymer Brushes as Neutral Surfaces for Controlling the Orientation of Block Copolymer Microdomains in Thin Films. *Langmuir* **2006**, *22*, 7855−7860.

(19) Bang, J.; Bae, J.; Löwenhielm, P.; Spiessberger, C.; Given-Beck, S. A.; Russell, T. P.; Hawker, C. J. Facile Routes to Patterned Surface Neutralization Layers for Block Copolymer Lithography. *Adv. Mater.* **2007**, *19*, 4552−4557.

(20) Ji, S.; Liu, C.-C.; Son, J. G.; Gotrik, K.; Craig, G. S. W.; Gopalan, P.; Himpsel, F. J.; Char, K.; Nealey, P. F. Generalization of the Use of Random Copolymers to Control the Wetting Behavior of Block Copolymer Films. *Macromolecules* **2008**, *41*, 9098−9103.

(21) Bates, C. M.; Strahan, J. R.; Santos, L. J.; Mueller, B. K.; Bamgbade, B. O.; Lee, J. A.; Katzenstein, J. M.; Ellison, C. J.; Willson, C. G. Polymeric Cross-Linked Surface Treatments for Controlling Block Copolymer Orientation in Thin Films. *Langmuir* **2011**, *27*, 2000−2006.

(22) Maher, M. J.; Bates, C. M.; Blachut, G.; Carlson, M. C.; Self, J. L.; Janes, D. W.; Durand, W. J.; Lane, A. P.; Ellison, C. J.; Willson, C. G. Photopatternable Interfaces for Block Copolymer Lithography. *ACS Macro Lett.* **2014**, 824−828.

(23) Seshimo, T.; Bates, C. M.; Dean, L. M.; Cushen, J. D.; Durand, W. J.; Maher, M. J.; Ellison, C. J.; Willson, C. G. Block Copolymer Orientation Control Using a Top-Coat Surface Treatment. *J. Photopolym. Sci. Technol.* **2012**, *25*, 125−130.

(24) Bates, C. M.; Seshimo, T.; Maher, M. J.; Durand, W. J.; Cushen, J. D.; Dean, L. M.; Blachut, G.; Ellison, C. J.; Willson, C. G. Polarity-Switching Top Coats Enable Orientation of Sub-10-nm Block Copolymer Domains. *Science* **2012**, *338*, 775−779.

(25) Yoshida, H.; Suh, H. S.; Ramirez-Herunandez, A.; Lee, J. I.; Aida, K.; Wan, L.; Ishida, Y.; Tada, Y.; Ruiz, R.; de Pablo, J.; Nealey, P. F. Topcoat Approaches for Directed Self-Assembly of Strongly Segregating Block Copolymer Thin Films. *J. Photopolym. Sci. Technol.* **2013**, *26*, 55−58.

(26) Bates, C. M.; Maher, M. J.; Thio, A.; Dean, L. M.; Cushen, J. D.; Durand, W. J.; Blachut, G.; Li, L.; Ellison, C. J.; Willson, C. G. Polarity-switching Top Coats for Silicon-containing Block Copolymer Orientation Control. *J. Photopolym. Sci. Technol.* **2013**, *26*, 223−224.

(27) Ramírez-Hernández, A.; Suh, H. S.; Nealey, P. F.; de Pablo, J. J. Control of Directed Self-Assembly in Block Polymers by Polymeric Topcoats. *Macromolecules* **2014**, *47*, 3520−3527.

(28) Mansky, P.; Russell, T. P.; Hawker, C. J.; Pitsikalis, M.; Mays, J. Ordered Diblock Copolymer Films on Random Copolymer Brushes. *Macromolecules* **1997**, *30*, 6810−6813.

(29) Peters, R. D.; Yang, X. M.; Nealey, P. F. Morphology of Thin Films of Diblock Copolymers on Surfaces Micropatterned with Regions of Different Interfacial Energy. *Macromolecules* **2002**, *35*, 1822−1834.

(30) Kim, S.; Bates, C. M.; Thio, A.; Cushen, J. D.; Ellison, C. J.; Willson, C. G.; Bates, F. S. Consequences of Surface Neutralization in Diblock Copolymer Thin Films. *ACS Nano* **2013**, *7*, 9905−9919.

(31) Maher, M. J.; Bates, C. M.; Blachut, G.; Sirard, S.; Self, J. L.; Carlson, M. C.; Dean, L. M.; Cushen, J. D.; Durand, W. J.; Hayes, C. O.; Ellison, C. J.; Willson, C. G. Interfacial Design for Block Copolymer Thin Films. *Chem. Mater.* **2014**, *26*, 1471−1479.

(32) Morkved, T. L.; Lu, M.; Urbas, A. M.; Ehrichs, E. E.; Jaeger, H. M.; Mansky, P.; Russell, T. P. Local Control of Microdomain

Orientation in Diblock Copolymer Thin Films with Electric Fields. *Science* **1996**, *273*, 931−933.
(33) Rockford, L.; Liu, Y.; Mansky, P.; Russell, T. P.; Yoon, M.; Mochrie, S. G. J. Polymers on Nanoperiodic, Heterogeneous Surfaces. *Phys. Rev. Lett.* **1999**, *82*, 2602−2605.
(34) Bodycomb, J.; Funaki, Y.; Kimishima, K.; Hashimoto, T. Single-Grain Lamellar Microdomain From a Diblock Copolymer. *Macromolecules* **1999**, *32*, 2075−2077.
(35) Segalman, R. A.; Yokoyama, H.; Kramer, E. J. Graphoepitaxy of Spherical Domain Block Copolymer Films. *Adv. Mater.* **2001**, *13*, 1152−1155.
(36) Cheng, J. Y.; Ross, C. A.; Thomas, E. L.; Smith, H. I.; Vancso, G. J. Fabrication of Nanostructures with Long-Range Order Using Block Copolymer Lithography. *Appl. Phys. Lett.* **2002**, *81*, 3657−3659.
(37) Yang, X. M.; Peters, R. D.; Nealey, P. F.; Solak, H. H.; Cerrina, F. Guided Self-Assembly of Symmetric Diblock Copolymer Films on Chemically Nanopatterned Substrates. *Macromolecules* **2000**, *33*, 9575−9582.
(38) Ouk Kim, S.; Solak, H. H.; Stoykovich, M. P.; Ferrier, N. J.; de Pablo, J. J.; Nealey, P. F. Epitaxial Self-Assembly of Block Copolymers on Lithographically Defined Nanopatterned Substrates. *Nature* **2003**, *424*, 411−414.
(39) Ruiz, R.; Kang, H.; Detcheverry Francois, A.; Dobisz, E.; Kercher, D. S.; Albrecht, T. R.; de Pablo, J. J.; Nealey, P. F. Density Multiplication and Improved Lithography by Directed Block Copolymer Assembly. *Science* **2008**, *321*, 936−939.
(40) Doerk, G. S.; Liu, C.-C.; Cheng, J. Y.; Rettner, C. T.; Pitera, J. W.; Krupp, L. E.; Topuria, T.; Arellano, N.; Sanders, D. P. Pattern Placement Accuracy in Block Copolymer Directed Self-Assembly Based on Chemical Epitaxy. *ACS Nano* **2013**, *7*, 276−285.
(41) Stoykovich, M. P.; Mueller, M.; Kim, S. O.; Solak, H. H.; Edwards, E. W.; de Pablo, J. J.; Nealey, P. F. Directed Assembly of Block Copolymer Blends Into Nonregular Device-Oriented Structures. *Science* **2005**, *308*, 1442−1446.
(42) Doerk, G. S.; Cheng, J. Y.; Rettner, C. T.; Balakrishnan, S.; Arellano, N.; Sanders, D. P. Deterministically Isolated Gratings Through the Directed Self-Assembly of Block Copolymers. *Proc. SPIE* **2013**, *8680*, 86800Y.
(43) Chang, J.-B.; Choi, H. K.; Hannon, A. F.; Alexander-Katz, A.; Ross, C. A.; Berggren, K. K. Design Rules for Self-Assembled Block Copolymer Patterns Using Tiled Templates. *Nat. Commun.* **2014**, *5*, 3305.
(44) Tsai, H.; Pitera, J. W.; Miyazoe, H.; Bangsaruntip, S.; Engelmann, S. U.; Liu, C.-C.; Cheng, J. Y.; Bucchignano, J. J.; Klaus, D. P.; Joseph, E. A.; Sanders, D. P.; Colburn, M. E.; Guillorn, M. A. Two-Dimensional Pattern Formation Using Graphoepitaxy of PS- *b*-PMMA Block Copolymers for Advanced FinFET Device and Circuit Fabrication. *ACS Nano* **2014**, *8*, 5227−5232.
(45) Cheng, J. Y.; Sanders, D. P.; Truong, H. D.; Harrer, S.; Friz, A.; Holmes, S.; Colburn, M.; Hinsberg, W. D. Simple and Versatile Methods to Integrate Directed Self-Assembly with Optical Lithography Using a Polarity-Switched Photoresist. *ACS Nano* **2010**, *4*, 4815−4823.
(46) Liu, C.-C.; Nealey, P. F.; Raub, A. K.; Hakeem, P. J.; Brueck, S. R. J.; Han, E.; Gopalan, P. Integration of Block Copolymer Directed Assembly with 193 Immersion Lithography. *J. Vac. Sci. Technol., B* **2010**, *28*, C6B30−C6B34.
(47) Liu, C.-C.; Thode, C. J.; Rincon Delgadillo, P. A.; Craig, G. S. W.; Nealey, P. F.; Gronheid, R. Towards an All-Track 300 mm Process for Directed Self-Assembly. *J. Vac. Sci. Technol., B* **2011**, *29*, 06F203.
(48) Delgadillo, P. R.; Gronheid, R.; Thode, C. J.; Wu, H.; Yi, C.; Neisser, M.; Somervell, M.; Nafus, K.; Nealey, P. F. Implementation of a Chemo-Epitaxy Flow for Directed Self-Assembly on 300-mm Wafer Processing Equipment. *J. Micro/Nanolithogr., MEMS, MOEMS* **2012**, *11*, 031302.
(49) Gronheid, R. Frequency Multiplication of Lamellar Phase Block Copolymers with Grapho-Epitaxy Directed Self-Assembly Sensitivity to Prepattern. *J. Micro/Nanolithogr., MEMS, MOEMS* **2012**, *11*, 031303.
(50) Delgadillo, P. R.; Suri, M.; Durant, S.; Cross, A.; Nagaswami, V. R.; Van Den Heuvel, D.; Gronheid, R.; Nealey, P. Defect Source Analysis of Directed Self-Assembly Process. *J. Micro/Nanolithogr., MEMS, MOEMS.* **2013**, *12*, 031112.
(51) Mansky, P.; Russell, T. P.; Hawker, C. J.; Mays, J.; Cook, D. C.; Satija, S. K. Interfacial Segregation in Disordered Block Copolymers: Effect of Tunable Surface Potentials. *Phys. Rev. Lett.* **1997**, *79*, 237−240.
(52) Liu, Y.; Longo, D. M.; Hull, R. Ultrarapid Nanostructuring of Poly(Methylmethacrylate) Films Using Ga^+ Focused Ion Beams. *Appl. Phys. Lett.* **2003**, *82*, 346.
(53) Zhao, Y.; Sivaniah, E.; Hashimoto, T. SAXS Analysis of the Order-Disorder Transition and the Interaction Parameter of Polystyrene-*block*-poly(methyl methacrylate). *Macromolecules* **2008**, *41*, 9948−9951.
(54) Durand, W. J.; Blachut, G.; Maher, M. J.; Sirard, S.; Tein, S.; Carlson, M. C.; Asano, Y.; Zhou, S. X.; Lane, A. P.; Bates, C. M.; Ellison, C. J.; Willson, C. G. Design of High-χ Block Copolymers for Lithography. *J. Polym. Sci., Part A: Polym. Chem.* **2015**, *53*, 344−352.
(55) Grigorescu, A. E.; van der Krogt, M. C.; Hagen, C. W.; Kruit, P. 10nm Lines and Spaces Written in HSQ, Using Electron Beam Lithography. *Microelectron. Eng.* **2007**, *84*, 822−824.
(56) Cheng, J. Y.; Rettner, C. T.; Sanders, D. P.; Kim, H.-C.; Hinsberg, W. D. Dense Self-Assembly on Sparse Chemical Patterns: Rectifying and Multiplying Lithographic Patterns Using Block Copolymers. *Adv. Mater.* **2008**, *20*, 3155−3158.
(57) Liu, C.-C.; Ramírez-Hernández, A.; Han, E.; Craig, G. S. W.; Tada, Y.; Yoshida, H.; Kang, H.; Ji, S.; Gopalan, P.; de Pablo, J. J.; Nealey, P. F. Chemical Patterns for Directed Self-Assembly of Lamellae-Forming Block Copolymers with Density Multiplication of Features. *Macromolecules* **2013**, *46*, 1415−1424.
(58) Hinsberg, W.; Cheng, J.; Kim, H.-C.; Sanders, D. P. Self-Assembling Materials for Lithographic Patterning: Overview, Status, and Moving Forward. *Proc. SPIE* **2010**, *7637*, 76370G.
(59) Farrell, R. A.; Hosler, E. R.; Schmid, G. M.; Xu, J.; Preil, M. E.; Rastogi, V.; Mohanty, N.; Kumar, K.; Cicoria, M. J.; Hetzer, D. R.; Devilliers, A. J. Manufacturability Considerations for DSA. *Proc. SPIE* **2014**, *9051*, 90510Z.
(60) Park, S. M.; Stoykovich, M. P.; Ruiz, R.; Zhang, Y.; Black, C. T.; Nealey, P. F. Directed Assembly of Lamellae- Forming Block Copolymers by Using Chemically and Topographically Patterned Substrates. *Adv. Mater.* **2007**, *19*, 607−611.

DOI: 10.1021/am508197k
ACS Appl. Mater. Interfaces 2015, 7, 3323−3328